MOEA/VAN: Multiobjective Evolutionary Algorithm Based on Vector Angle Neighborhood

Roman Denysiuk
Algoritmi R&D Center
University of Minho
Campus de Gualtar
4710-057 Braga, Portugal
roman.denysiuk@algoritmi.uminho.pt

Lino Costa
Department of Production and Systems Engineering
University of Minho
Campus de Gualtar
4710-057 Braga, Portugal
lac@dps.uminho.pt

Isabel Espírito Santo
Department of Production and Systems Engineering
University of Minho
Campus de Gualtar
4710-057 Braga, Portugal
iapinho@dps.uminho.pt

ABSTRACT

Natural selection favors the survival and reproduction of organisms that are best adapted to their environment. Selection mechanism in evolutionary algorithms mimics this process, aiming to create environmental conditions in which artificial organisms could evolve solving the problem at hand. This paper proposes a new selection scheme for evolutionary multiobjective optimization. The similarity measure that defines the concept of the neighborhood is a key feature of the proposed selection. Contrary to commonly used approaches, usually defined on the basis of distances between either individuals or weight vectors, it is suggested to consider the similarity and neighborhood based on the angle between individuals in the objective space. The smaller the angle, the more similar individuals. This notion is exploited during the mating and environmental selections. The convergence is ensured by minimizing distances from individuals to a reference point, whereas the diversity is preserved by maximizing angles between neighboring individuals. Experimental results reveal a highly competitive performance and useful characteristics of the proposed selection. Its strong diversity preserving ability allows to produce a significantly better performance on some problems when compared with stat-of-the-art algorithms.

Categories and Subject Descriptors

I.2.8 [**Artificial Intelligence**]: Problem Solving, Control Methods, and Search–*Heuristic methods*

Keywords

Multiobjective optimization; Evolutionary multiobjective optimization; Multiobjective evolutionary algorithms; Performance assessment

GECCO '15, July 11 - 15, 2015, Madrid, Spain

DOI: http://dx.doi.org/10.1145/2739480.2754722

1. INTRODUCTION

In practice, the simultaneous optimization of multiple objectives has become widespread. Without loss of generality, a multiobjective optimization problem (MOP) with m objectives and n decision variables can be formulated as:

$$\begin{array}{rl} \text{minimize:} & \boldsymbol{f}(\boldsymbol{x}) = (f_1(\boldsymbol{x}), f_2(\boldsymbol{x}), \ldots, f_m(\boldsymbol{x}))^{\mathrm{T}} \\ \text{subject to:} & \boldsymbol{x} \in \Omega \end{array} \tag{1}$$

where $\boldsymbol{x}$ is the decision vector, $\Omega \subseteq \mathbb{R}^n$ is the feasible decision space, and $\boldsymbol{f}(\boldsymbol{x})$ is the objective vector defined in the attainable objective space $\Theta \subseteq \mathbb{R}^m$.

In multiobjective optimization, the Pareto dominance relation is usually used to define the concepts of optimality. For two solutions $\boldsymbol{x}$ and $\boldsymbol{y}$ from Ω, a solution $\boldsymbol{x}$ is said to dominate a solution $\boldsymbol{y}$ (denoted by $\boldsymbol{x} \prec \boldsymbol{y}$) if for all $i \in \{1, \ldots, m\}$ $f_i(\boldsymbol{x}) \leq f_i(\boldsymbol{y})$ and there exists at least one objective such that $f_j(\boldsymbol{x}) < f_j(\boldsymbol{y})$.

A solution $\boldsymbol{x}^* \in \Omega$ is Pareto optimal if and only if:

$$\nexists \boldsymbol{y} \in \Omega : \boldsymbol{y} \prec \boldsymbol{x}^*. \tag{2}$$

In the presence of multiple conflicting objectives, there is a set of optimal solutions, known as the Pareto optimal set. For MOP (1), the Pareto optimal set (or Pareto set for short) is defined as:

$$\mathcal{PS} = \{\boldsymbol{x}^* \in \Omega \,|\, \nexists \boldsymbol{y} \in \Omega : \boldsymbol{y} \prec \boldsymbol{x}^*\}. \tag{3}$$

For MOP (1) and the Pareto set $\mathcal{PS}$, the Pareto optimal front (or Pareto front for short) is defined as:

$$\mathcal{PF} = \{\boldsymbol{f}(\boldsymbol{x}^*) \in \Theta \,|\, \boldsymbol{x}^* \in \mathcal{PS}\}. \tag{4}$$

Since it is often not possible to obtain the whole Pareto set, solving (1) is usually understood as approximating the Pareto set by obtaining a set of solutions that are as close as possible to the Pareto set and as diverse as possible.

Evolutionary algorithms (EAs) have become popular in solving MOPs. Similarly to single-objective counterparts, multiobjective evolutionary algorithms (MOEAs) draw inspiration from natural evolution. Natural selection is responsible for adaptation of species to their environment, giving extra survival and reproduction probability to the most fitted individuals. EAs usually mimic this process by assigning fitness values to population members and sampling the population, according to these values. Although it can be relatively easy in the single-objective case, it is not so straightforward in multiobjective optimization. Therefore, selection is a major issue in the design of MOEAs.

Based on the fitness assignment and selection, most modern MOEAs can be classified into three major categories: dominance-, scalarizing- and indicator-based algorithms. Dominance-based MOEAs use the concept of the Pareto dominance. To guide the search, the dominance relation between population members and the population diversity can be incorporated in a scalar fitness value [21]. Another common approach is to perform two stage selection, ranking and selection individuals according to nondomination levels and applying diversity preserving mechanism when the last accepted level cannot be completely accommodated [3]. Due to a low selection pressure in high dimensional objective spaces, the performance of dominance-based algorithms severely deteriorates when the number of objectives is increased [15]. This issue can be addressed by modifying the dominance relation [16, 19] or the diversity preserving mechanism [5, 6, 12]. For some other problems, the dominance relation provides a high selection pressure [11], which can be harmful for search due to the loss of diversity. Scalarizing-based approaches incorporate traditional mathematical techniques [14] based on the aggregation of multiple objectives into a single parameterized function. A scalar fitness value is assigned to each population member, with an individual representing a solution to the corresponding single-objective function. MOEAs relying on scalarization produce promising results for many-objective problems [9] and in terms of balancing the convergence and diversity [11]. Though this balance cannot be ensured on some other problems [13]. To use scalarizing functions, a set of weight vectors usually must be provided in advance, which is not easy for all the cases. To guide the search, indicator-based approaches employ performance indicators, such as the ϵ or hypervolume indicators. A scalar fitness value is assigned to each population member, reflecting its quality with respect to the convergence and diversity [20]. Indicator-based MOEAs are successful in dealing with many-objective problems [17]. The difficulty in their application arises from the high computational cost. For example, the time required for calculating the hypervolume grows exponentially with the number of objectives [18], limiting significantly its applicability. Approximating the hypervolume requires the compromise between accuracy and complexity [1].

This study suggests a selection scheme that does not rely on the aforementioned fitness assignment strategies. The proposed framework shares some similarities with MOEA/D, being different in several ways. MOEA/VAN does not require a prior information in terms of weight vectors, alleviating user's burden. Its selection scheme is adaptive and solely based on interactions between individuals in the current population. The concept of the similarity is defined based on the angle between objective vectors. MOEA/VAN attempts to maintain the population as diverse as possible, according to the defined measure. One of the two most similar individuals in the population is removed, according to the convergence. As a result, less selection pressure and higher diversity are expected, which can be beneficial for search.

The remainder of this paper is organized as follows. Section 2 describes the proposed framework. Section 3 reports results of the experimental study, including experimentation with different configurations and comparison with state-of-the-art algorithms. Section 4 concludes the study and outlines some possible future work.

2. PROPOSED FRAMEWORK

Multiobjective evolutionary algorithm based on vector angle neighborhood (MOEA/VAN) solves a multiobjective optimization problem by minimizing distances between population members and a reference point while maximizing angles between neighboring individuals. Contrary to MOEAs, which minimize a weighted distance to a reference point [11], MOEA/VAN does not require a set of weight vectors to be provided beforehand.

During the search, MOEA/VAN maintains the population, P, of size μ and a reference point, $\boldsymbol{z}$, composed of the lowest objective values found so far. Each individual in P is represented by the decision vector $\boldsymbol{x}$, the vector of objective functions $\boldsymbol{f}$, the vector of translated objectives $\tilde{\boldsymbol{f}}$ calculated as:

$$\tilde{f}_j = f_j - z_j \quad \forall j \in \{1, \dots, m\} \tag{5}$$

and the vector $\boldsymbol{\theta}$ containing all the angles between the current individual and the other population members. During the evolution, translated objective values, $\tilde{\boldsymbol{f}}$, are used. The angle between the individuals a and b is computed as:

$$\theta = \arccos\left(\frac{\langle \tilde{\boldsymbol{f}}_a, \tilde{\boldsymbol{f}}_b \rangle}{\|\tilde{\boldsymbol{f}}_a\| \|\tilde{\boldsymbol{f}}_b\|}\right) \tag{6}$$

where $\langle \cdot, \cdot \rangle$ denotes the dot product and $\| \cdot \|$ denotes the Euclidean norm.

The convergence is ensured by minimizing the p-norm of each individual:

$$\|\tilde{\boldsymbol{f}}\|_p = \left(\sum_{j=1}^{m} |\tilde{f}_j|^p\right)^{\frac{1}{p}}. \tag{7}$$

For preserving diversity, one of the two most similar individuals in the population is removed after generating offspring. As the similarity measure defying the concept of the neighborhood, the angle between individuals is used. The smaller the angle, the closer (or more similar) individuals. It is important to note that the length of vectors and the distance between them do not play a major role for defining similarity. Due to these features, it is expected that the selection would be particularly useful for maintaining diversity and not be affected by the curse of dimensionality.

In this study, the real representation for individuals is used. An offspring individual, $\boldsymbol{y}$, is produced using a differential evolution (DE) operator that works as follows $\forall j \in \{1, \dots, n\}$:

$$y_j = \begin{cases} x_j^i + F \times (x_j^{r1} - x_j^{r2}) & \text{with probability } CR \\ x_j^i & \text{with probability } 1 - CR \end{cases} \tag{8}$$

The polynomial mutation is applied on the offspring as follows $\forall j \in \{1, \dots, n\}$:

$$y_j = \begin{cases} y_j + \sigma_j \times (ub_j - lb_j) & \text{with probability } p_m \\ y_j & \text{with probability } 1 - p_m \end{cases} \tag{9}$$

where lb_j and ub_j are the lower and upper bounds of the j-th variable, respectively,

$$\sigma_j = \begin{cases} (2u_j)^{1/(1+\eta_m)} - 1 & \text{if } u_j \leq 0.5 \\ 1 - (2 - 2u_j)^{1/(1+\eta_m)} & \text{otherwise} \end{cases} \tag{10}$$

and $u_j \in [0, 1]$ is a uniform random number. To ensure feasibility, individuals are repaired as:

$$y_j = \min\{\max\{y_j, lb_j\}, ub_j\} \quad \forall j \in \{1, \dots, n\}. \tag{11}$$

The outline of MOEA/VAN is given as follows:

Input:

- CR - crossover probability;
- F - scaling factor;
- p_m - mutation probability;
- η_m - mutation distribution index;
- δ - probability for mating pool;
- T - neighborhood size for mating selection;
- K - neighborhood size for environmental selection;
- p - parameter defining p-norm;
- μ - population size;
- $maxEval$ - maximum number of function evaluations.

Output:

- $\{\boldsymbol{x}^1, \ldots, \boldsymbol{x}^\mu\}$ - approximation to the Pareto set;
- $\{\boldsymbol{f}(\boldsymbol{x}^1), \ldots, \boldsymbol{f}(\boldsymbol{x}^\mu)\}$ - approximation to the Pareto front.

Step 1 Initialization

Step 1.1 Randomly generate initial population.

Step 1.2 Initialize a reference point, $\boldsymbol{z}$, as $\forall j \in \{1, \ldots, m\}$: $z_j = \min_{1 \leq i \leq \mu} f_j(\boldsymbol{x}^i)$

Step 1.3 Translate objective vectors using (5).

Step 1.4 Compute the angles between all the population members using (6).

Step 2 Mating selection

Step 2.1 Uniformly at random select a population member (say the i-th individual is selected).

Step 2.2 With probability δ, select two different individuals $r1$ and $r2$ from the T closest individuals, or with probability $(1 - \delta)$ select these individuals from the whole population.

Step 3 Variation

Step 3.1 Generate an offspring, $\boldsymbol{y}$, using a differential evolution (DE) operator.

Step 3.2 Apply polynomial mutation on the offspring.

Step 3.3 Repair the offspring.

Step 4 Update

Step 4.1 For each $j \in \{1, \ldots, m\}$, if $f_j(\boldsymbol{y}) < z_j$, then set $z_j = f_j(\boldsymbol{y})$.

Step 4.2 If $\boldsymbol{z}$ was updated in Step 4.1, translate objectives for $P \cup \boldsymbol{y}$. Otherwise, translate objectives for $\boldsymbol{y}$.

Step 4.3 If $\boldsymbol{z}$ was updated in Step 4.1, compute the angles between all the members of $P \cup \boldsymbol{y}$. Otherwise, compute the angles between $\boldsymbol{y}$ and all the members of P.

Step 5 Environmental selection

Step 5.1 If $\boldsymbol{y}$ is better for at least one objective comparing with each of K closest individuals in the population, go to Step 5.2. Otherwise, go to **Step 6**.

Step 5.2 Find two closest individuals from $P \cup \boldsymbol{y}$, and remove individual having larger $\|\tilde{f}\|_p$.

Step 6 If the maximum number of function evaluations is reached, then stop. Otherwise, go to **Step 2**.

3. EXPERIMENTAL VALIDATION

This section presents and discusses results of the experimental study carried out to validate the proposed approach. The experimental study is divided into two parts, which are devoted to handling different problem characteristics. For experiments, GDE3 [10], MOEA/D [11] and IBEA [20] are used within the JMetal framework [7]. The major reason for choosing these algorithms is that they are established state-of-the-art algorithms and represent the main trends to the fitness assignment and selection in MOEAs – namely the dominance-, scalarizing- and indicator-based strategies. Hence, they serve as an important reference for evaluating the proposed approach, where the main novelty is the selection mechanism.

3.1 Complicated Pareto Sets

In this part, two sets of challenging problems from [11] and [13] are adopted, which are referred in the following as the LZ09 and LGZ test suites, respectively. These problems pose significant difficulties for MOEAs in terms of obtaining well distributed approximations. First, experiments are conducted to estimate the effects of major control parameters in MOEA/VAN. Then, the performance of MOEA/VAN is compared with state-of-the-art algorithms.

3.1.1 Experimental Setup

The values of δ, T, K and p for MOEA/VAN are determined in parametrization study. Some general parameters are as shown in Table 1. The remaining settings are as follows. Thirty independent runs are performed with a population size of $\mu = 300$, running for 1.5×10^5 and 3×10^5 function evaluations on the LZ09 and LGZ problems, respectively. These settings are as suggested in [11] and [13].

MOEA/VAN	MOEA/D	GDE3	IBEA
$CR = 1.0$ $F = 0.5$ $\eta_m = 20$ $p_m = 1/n$	$CR = 1.0$ $F = 0.5$ $\eta_m = 20$ $p_m = 1/n$ $\delta = 0.9$ $T = 20$	$CR = 1.0$ $F = 0.5$ $\eta_m = 20$ $p_m = 1/n$	$\eta_c = 20$ $p_c = 0.9$ $\eta_m = 20$ $p_m = 1/n$

Table 1: Parameter settings for the algorithms.

As the performance measure, the inverted generational distance (IGD) indicator [2] is used. This indicator can be referred as the distance from the Pareto front, $\mathcal{PF}$, to an approximation set [23], A. IGD can be defined as:

$$I_{IGD} = \frac{\sum_{\boldsymbol{a}' \in \mathcal{PF}} d(\boldsymbol{a}', A)}{|\mathcal{PF}|} \tag{12}$$

where $d(\boldsymbol{a}', A)$ is the minimum Euclidean distance between $\boldsymbol{a}'$ and the points in A. IGD can measure both the diversity and convergence of A. The smaller the value of I_{IGD}, the better the quality of A. For calculating IGD, 1,000 uniformly distributed points along the Pareto front are generated for each problem. For statistically sound conclusions, the Wilcoxon rank sum test is performed at significance level of 0.05 [8].

3.1.2 Parametrization Study

MOEA/VAN relies on the setting of δ, T during the mating selection and K, p during the environmental selection.

δ \ T	10	20	30	40
0.7	5.67	3.33	8.78	10.33
0.8	5.78	4.67	7.11	10.67
0.9	9.33	5.56	7.00	9.56
1.0	13.22	11.33	11.33	12.33

(a) LZ09 test suite

δ \ T	10	20	30	40
0.7	9.57	8.14	11.43	13.57
0.8	8.71	5.00	9.71	12.71
0.9	8.43	2.71	6.43	10.71
1.0	11.57	2.43	6.00	8.86

(b) LGZ test suite

δ \ T	10	20	30	40
0.7	7.38	5.44	9.94	11.75
0.8	7.06	4.81	8.25	11.56
0.9	8.94	4.31	6.75	10.06
1.0	12.50	7.44	9.00	10.81

(c) LZ09 and LGZ test suites

Table 2: Mean ranks for different values of δ and T.

p \ K	0	1	5	300
1.0	4.78	3.44	6.78	11.78
2.0	5.00	3.67	7.22	12.33
10.0	9.22	5.78	10.11	13.44
∞	10.00	7.33	11.11	14.00

(a) LZ09 test suite

p \ K	0	1	5	300
1.0	7.00	2.71	7.71	15.14
2.0	6.43	2.14	8.29	14.14
10.0	7.43	4.00	9.00	14.29
∞	8.43	5.71	9.14	14.43

(b) LGZ test suite

p \ K	0	1	5	300
1.0	5.75	3.13	7.19	13.25
2.0	5.63	3.00	7.69	13.13
10.0	8.44	5.00	9.63	13.81
∞	9.31	6.63	10.25	14.19

(c) LZ09 and LGZ test suites

Table 3: Mean ranks for different values of p and K.

These are the major control parameters that determine the performance of the algorithm. To investigate the sensitivity of MOEA/VAN to these parameters, the following experiments are performed.

First, the performance of MOEA/VAN is studied for $\delta \in \{0.7, 0.8, 0.9, 1.0\}$ and $T \in \{10, 20, 30, 40\}$. Table 2 shows the results with respect to IGD. It can be seen that MOEA/VAN is not very sensitive to these parameters, with $T = 20$ being the best choice. Concerning δ, results indicate that MOEA/VAN must focus more on exploration for LZ09 and exploitation for LGZ.

Further, the performance of MOEA/VAN is studied for $p \in \{1, 2, 10, \infty\}$ and $K \in \{0, 1, 5, 300\}$. The obtained results are presented in Table 3. These results also indicate that MOEA/VAN is not very sensitive to the choice of p and K, with $K = 1$ being the best setting for the LZ09 and LGZ suites along with $p = 1$ and $p = 2$ that are notably better than other values. Based on the obtained results, in the following experiments, MOEA/VAN is used with $\delta = 0.9$, $T = 20$, $p = 2$ and $K = 1$.

3.1.3 *Comparison Study*

The main focus of this study is to evaluate the competitiveness of the selection scheme used in MOEA/VAN when dealing with problems that pose significant challenge for many MOEAs to obtain a well converged and distributed approximations. Table 4 shows the results obtained on the LZ09 and LGZ problems. The results indicate that MOEA/D dominates the other algorithms on the LZ09 problems. It should be noted that MOEA/VAN also provides a highly competitive performance on these instances. MOEA/VAN always performs better than GDE3 and IBEA. Also, it is statistically better than the other three algorithms on F6. This can be further confirmed when looking at Figure 1, which shows approximation sets with the best IGD values obtained by MOEA/VAN. From the plots, it is clear that MOEA/VAN is able to obtain adequate approximations for all these problems. Concerning the LGZ problems, MOEA/VAN clearly outperforms all the other algorithms, being statistically better with respect to IGD on all the instances.

To explain the much better performance of MOEA/VAN on the LGZ suite, 10^4 points are randomly generated in the decision space using the Latin hypercube sampling. Figure 2 illustrates their mapping into the objective space for F1. The plot suggests a significant bias in the fitness landscape. A large number of points are located close to the corner point of the Pareto front. Whereas points that occupy intermediate regions of the objective space are far away from the Pareto front and are dominated by those points in

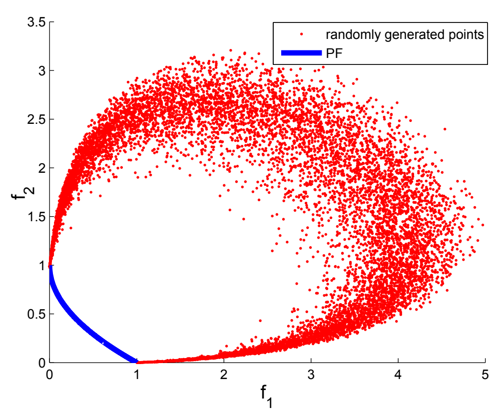

Figure 2: Image of 10^4 evenly distributed points in the decision space for LGZ1.

	MOEA/VAN	MOEA/D	GDE3	IBEA
F1	2.15e-03 (9.1e-05)$^{\mathrm{III,IV}}$	1.31e-03 (7.7e-06)$^{\mathrm{I,III,IV}}$	2.19e-03 (1.0e-04)$^{\mathrm{IV}}$	6.77e-03 (7.4e-04)
F2	4.40e-03 (9.5e-04)$^{\mathrm{III,IV}}$	2.75e-03 (2.8e-04)$^{\mathrm{I,III,IV}}$	4.23e-02 (5.2e-03)$^{\mathrm{IV}}$	1.12e-01 (1.5e-02)
F3	9.20e-03 (1.1e-02)$^{\mathrm{III,IV}}$	2.69e-03 (4.2e-03)$^{\mathrm{I,III,IV}}$	3.66e-02 (2.7e-03)$^{\mathrm{IV}}$	5.48e-02 (2.9e-02)
F4	1.00e-02 (5.6e-03)$^{\mathrm{III,IV}}$	6.46e-03 (9.9e-03)$^{\mathrm{I,III,IV}}$	3.62e-02 (3.4e-03)$^{\mathrm{IV}}$	7.14e-02 (4.3e-02)
F5	1.56e-02 (6.4e-03)$^{\mathrm{III,IV}}$	1.22e-02 (5.4e-03)$^{\mathrm{I,III,IV}}$	3.53e-02 (4.4e-03)$^{\mathrm{IV}}$	3.96e-02 (1.5e-02)
F6	3.11e-02 (5.3e-04)$^{\mathrm{II,III,IV}}$	4.69e-02 (8.9e-03)$^{\mathrm{III,IV}}$	1.14e-01 (2.3e-02)$^{\mathrm{IV}}$	5.33e-01 (4.6e-02)
F7	1.99e-03 (1.1e-04)$^{\mathrm{III,IV}}$	1.34e-03 (2.1e-05)$^{\mathrm{I,III,IV}}$	3.94e-01 (0.0e+00)	1.98e-01 (9.1e-02)$^{\mathrm{III}}$
F8	3.78e-03 (5.8e-03)$^{\mathrm{III,IV}}$	1.71e-03 (1.8e-03)$^{\mathrm{I,III,IV}}$	3.94e-01 (0.0e+00)	2.07e-01 (4.5e-02)$^{\mathrm{III}}$
F9	4.42e-03 (2.1e-03)$^{\mathrm{III,IV}}$	3.85e-03 (2.1e-03)$^{\mathrm{I,III,IV}}$	4.50e-02 (7.8e-03)$^{\mathrm{IV}}$	1.20e-01 (6.7e-02)

(a) LZ09 test suite

	MOEA/VAN	MOEA/D	GDE3	IBEA
F1	1.62e-02 (3.6e-03)$^{\mathrm{II,III,IV}}$	3.52e-01 (1.4e-02)$^{\mathrm{III,IV}}$	3.60e-01 (1.1e-02)	3.58e-01 (5.7e-03)
F2	3.55e-03 (1.3e-02)$^{\mathrm{II,III,IV}}$	2.08e-01 (6.3e-02)$^{\mathrm{III,IV}}$	3.55e-01 (0.0e+00)$^{\mathrm{IV}}$	3.55e-01 (5.6e-17)
F3	5.68e-03 (1.9e-02)$^{\mathrm{II,III,IV}}$	4.33e-01 (2.2e-02)$^{\mathrm{III}}$	5.02e-01 (7.1e-02)	4.55e-01 (6.6e-02)$^{\mathrm{III}}$
F4	1.38e-02 (1.1e-02)$^{\mathrm{II,III,IV}}$	2.25e-01 (7.8e-03)	2.18e-01 (3.7e-02)$^{\mathrm{II}}$	2.22e-01 (7.4e-03)$^{\mathrm{II}}$
F5	1.54e-02 (2.0e-03)$^{\mathrm{II,III,IV}}$	3.18e-01 (7.6e-03)	3.03e-01 (2.6e-02)$^{\mathrm{II}}$	2.45e-01 (2.6e-02)$^{\mathrm{II,III}}$
F6	5.79e-02 (2.6e-03)$^{\mathrm{II,III,IV}}$	3.19e-01 (8.5e-08)	3.19e-01 (2.6e-02)$^{\mathrm{II,IV}}$	3.19e-01 (7.1e-06)$^{\mathrm{II}}$
F7	1.20e-01 (4.7e-03)$^{\mathrm{II,III,IV}}$	4.01e-01 (2.0e-02)$^{\mathrm{IV}}$	4.01e-01 (3.2e-06)$^{\mathrm{IV}}$	4.04e-01 (1.0e-03)

(b) LGZ test suite

Table 4: Median and interquartile range of the IGD indicator. The superscripts I, II, III and IV indicate whether the respective algorithm performs statistically better than MOEA/VAN, MOEA/D, GDE3 and IBEA, respectively.

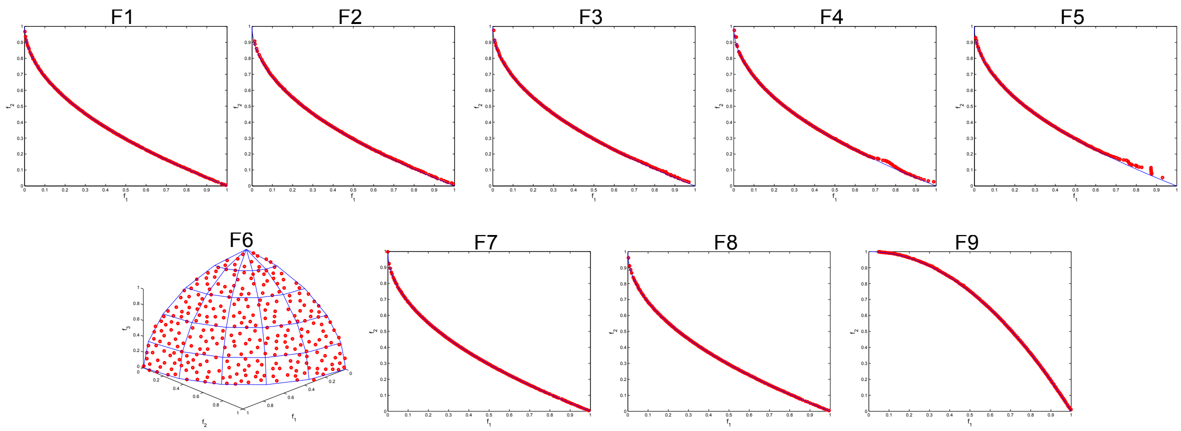

Figure 1: Approximation sets for the LZ09 test suite obtained by MOEA/VAN.

the extreme regions of the Pareto front. From the earliest generations, individuals located in the corner regions will be highly favored by the majority of selection schemes. The high selection pressure will filter out individuals in the other regions. The number of population members located close to the corner points of the Pareto front will grow, resulting in the severe loss of diversity and the stagnation of the population. Such circumstances require selection to tread the convergence and diversity equally.

Figure 3 presents the best approximations in terms of IGD obtained by all the algorithms for the LGZ problems. As expected, due to a poor ability to keep diversity in the above outlined environmental conditions, MOEA/D, IBEA and GDE3 located only those solutions that are close to the boundaries of the Pareto front. Whereas the remaining optimal regions are left unexplored, for the majority of cases.

On the other hand, MOEA/VAN is able to produce adequate approximations for all the instances. This is due to the proposed selection scheme that attempts to maximize angles between individuals, thereby forcing the uniform distribution of the population over the objective space. To replace some population member, a better converged individual must appear in the same region of the objective space. This guarantees that diverse individuals are not lost even though they appear unpromising comparing with other individuals, as exploitation of their diversity plays a crucial role for the population to evolve. Another nice feature of the MOEA/VAN selection scheme is that it is completely adaptive, being solely defined by the interplay between population members and the existing environment. Though it worth mentioning that the uniform distribution of angles does not guarantee the uniform distribution of approximation set, which can be largely influenced by the Pareto front geometry.

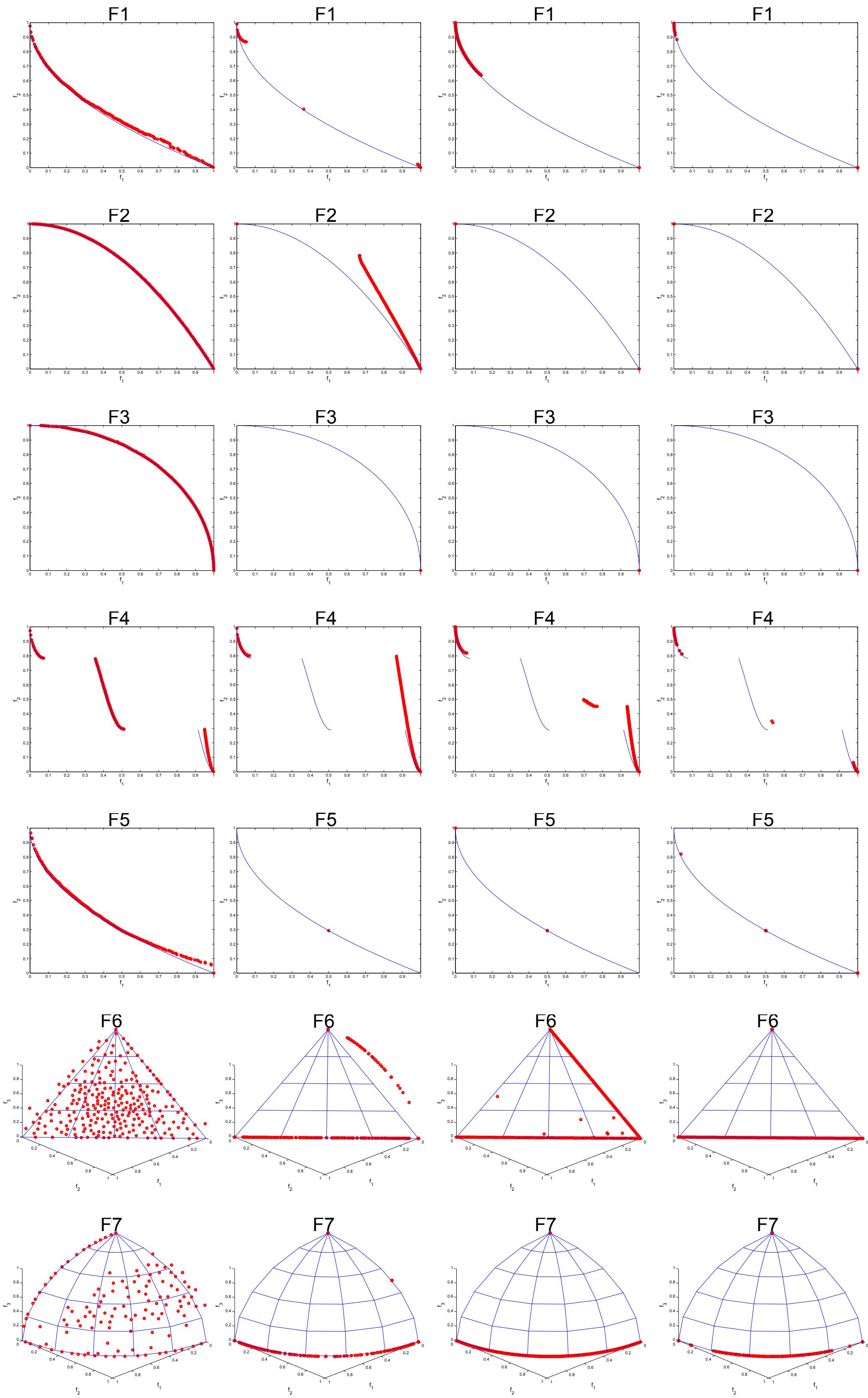

Figure 3: Approximation sets for the LGZ test suite obtained by MOEA/VAN, MOEA/D, GDE3 and IBEA, left to right.

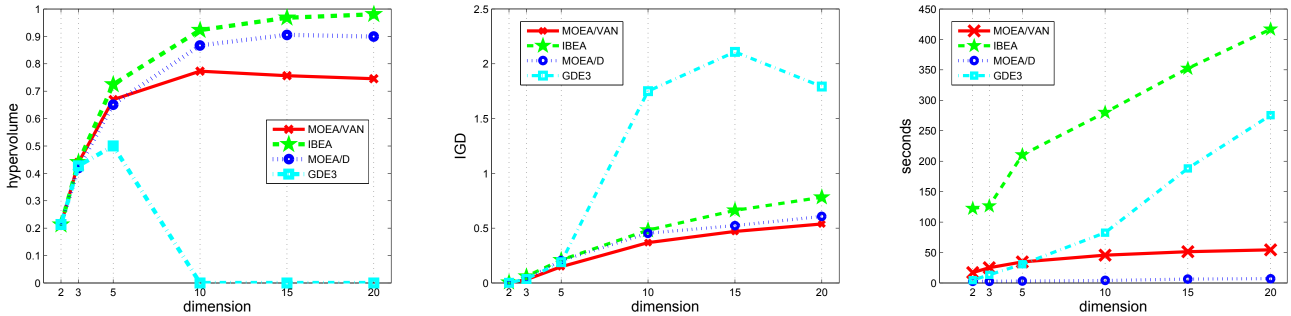

(a) HV (the higher the better) (b) IGD (the lower the better) (c) run time

Figure 4: Results for many-objective optimization.

3.2 Many-Objective Optimization

The issue of scalability of MOEAs has drawn considerable attention in recent years because many state-of-the-art algorithms face significant difficulties in dealing with many-objective problems, whereas those are widespread in practice. In the following, the performance of MOEA/VAN is studied in high dimensional objective spaces, adopting the DTLZ2 problem [4] for this purpose.

3.2.1 Experimental Setup

For the performance comparison, all algorithms are run on the DTLZ2 problem with the fixed number of decision variables, $n = 30$, ranging from 2 to 20 objectives. The population size is as in the previous experiments. The stopping criterion for state-of-the-art MOEAs is 500 generations, with MOEA/VAN run for equivalent number of function evaluations.

The outcomes are assessed using the IGD and hypervolume (HV) indicators. The hypervolume [22] can be defined as the Lebesgue measure, Λ, of the union of hypercuboids in the objective space:

$$I_H = \Lambda\left(\bigcup_{\boldsymbol{a}\in A}\{f_1(\boldsymbol{a}'),\ldots,f_m(\boldsymbol{a}') : \boldsymbol{a} \prec \boldsymbol{a}' \prec \boldsymbol{r}\}\right) \quad (13)$$

where $A = \{\boldsymbol{a}_1,\ldots,\boldsymbol{a}_{|A|}\}$ denotes a set of nondominated solutions and $\boldsymbol{r}$ is a reference point. The higher I_H, the better performance. For calculating the HV indicator, the nadir point is used as a reference point. Solutions that do not dominate the nadir point are discarded. If there is no solution dominating the nadir point, then the hypervolume of A is equal to zero. Solutions used to calculate the hypervolume are normalized using the ideal and nadir points [14].

3.2.2 Comparison Study

Figure 4 summarizes the results obtained for many-objective optimization. The graphical representation of the median values of the HV and IGD indicators are shown in Figures 4a and 4b, respectively. These plots reveal that the performance of MOEA/VAN is comparable with those produced by the established many-objective optimizers (IBEA and MOEA/D). Whereas the performance of GDE3 severely deteriorates when the number of objectives is increased. MOEA/VAN tends to maintain a uniform distribution of individuals in the population, this feature allows to obtain the best performance in terms of IGD up to 20 objectives (Figure 4b). With respect to the hypervolume, which is a biased indicator, IBEA achieves the best results followed by MOEA/D with the decomposition method based on the Chebyshev metric (Figure 4a). Nonetheless, it is clear that the selection in MOEA/VAN can guide the search in high dimensional objective spaces. Figure 4c presents the mean computational time consumed by the algorithms. This figure shows that MOEA/VAN consumes less time than IBEA and more time than MOEA/D. In turn, GDE3 works faster when the number of objectives is small and slower for high dimensional spaces. It can be seen that the computational time does not grow sharply with the number of objectives, as it is for IBEA and GDE3. The main computational burden in the selection of MOEA/VAN is incurred when a reference point has been updated and the update of angles between individuals is required, though it can be negligible in real-world applications. Thus, the obtained results appear encouraging for the use of MOEA/VAN in many-objective optimization.

4. CONCLUSIONS

Balancing the convergence and diversity is an important issue that must be taken into consideration when designing evolutionary algorithms for solving multiobjective optimization problems. This paper proposed a new selection scheme for evolutionary multiobjective optimization. To provide convergence, individuals in the population seek to minimize their distances to a reference point defined by the lowest objective values found during the search. After generating an offspring, closest neighbors in the population are compared to remove the inferior one with respect to convergence. As similarity measure that defines the concept of neighborhood, the angle between objective vectors is used.

MOEA/VAN is validated by performing the experimental study using test suites with different characteristics and state-of-the-art algorithms. The obtained results indicate that MOEA/VAN is not very sensitive to the choice of major control parameters, with the default settings being suggested. The results of the comparison study reveal a highly competitive performance of MOEA/VAN. Clear advantages of the proposed selection are observed on problems where the ability to keep diversity plays a crucial role. Also, encouraging results are obtained for problems with high dimensional objective spaces. Further attractive feature of the proposed selection is that it is completely adaptive and the need for user's interaction is minimized.

As future work, it is intended to address limitations of the proposed approach and further exploit its strengths. The selection in MOEA/VAN can face difficulties in handling problems with disconnected or degenerated Pareto fronts. One possible way to overcome this is to maintain an archive with nondominated solutions found during the search. Also, it would be interesting to investigate the MOEA/VAN framework combined with other offspring generating strategies and to design a more elaborate mating selection procedure. Further, MOEA/VAN can be extended from a steady-state to generation variant, as well as the adaptation of control parameters is another promising research direction.

5. ACKNOWLEDGMENTS

This work has been supported by FCT - Fundação para a Ciência e Tecnologia in the scope of the project: PEst-OE/EEI/UI0319/2014.

6. REFERENCES

[1] J. Bader and E. Zitzler. HypE: An algorithm for fast hypervolume-based many-objective optimization. *Evolutionary Computation*, 19(1):45–76, 2011.

[2] P. A. N. Bosman and D. Thierens. The balance between proximity and diversity in multiobjective evolutionary algorithms. *IEEE Transactions on Evolutionary Computation*, 7(2):174–188, 2003.

[3] K. Deb, A. Pratap, S. Agarwal, and T. Meyarivan. A fast and elitist multiobjective genetic algorithm: NSGA-II. *IEEE Transactions on Evolutionary Computation*, 6(2):182–197, 2002.

[4] K. Deb, L. Thiele, M. Laumanns, and E. Zitzler. Scalable test problems for evolutionary multi-objective optimization. Technical Report 112, Swiss Federal Institute of Technology, Zurich, Switzerland, 2001.

[5] R. Denysiuk, L. Costa, and I. Espírito Santo. Many-objective optimization using differential evolution with variable-wise mutation restriction. In *Proceedings of the Conference on Genetic and Evolutionary Computation*, GECCO'13, pages 591–598, 2013.

[6] R. Denysiuk, L. Costa, and I. Espírito Santo. Clustering-based selection for evolutionary many-objective optimization. In *Parallel Problem Solving from Nature*, PPSN'14, pages 538–547, 2014.

[7] J. J. Durillo and A. J. Nebro. jMetal: A Java framework for multi-objective optimization. *Advances in Engineering Software*, 42(10):760–771, 2011.

[8] S. García, D. Molina, M. Lozano, and F. Herrera. A study on the use of non-parametric tests for analyzing the evolutionary algorithms' behaviour: A case study on the CEC'2005 special session on real parameter optimization. *Journal of Heuristics*, 15(6):617–644, 2009.

[9] E. J. Hughes. Evolutionary many-objective optimisation: Many once or one many? In *Proceedings of the IEEE Congress on Evolutionary Computation*, CEC'05, pages 222–227, 2005.

[10] S. Kukkonen and J. Lampinen. GDE3: the third evolution step of generalized differential evolution. In *Proceedings of the IEEE Congress on Evolutionary Computation*, CEC'05, pages 443–450, 2005.

[11] H. Li and Q. Zhang. Multiobjective optimization problems with complicated Pareto sets, MOEA/D and NSGA-II. *IEEE Transactions on Evolutionary Computation*, 13(2):284–302, 2009.

[12] M. Li, S. Yang, and X. Liu. Shift-based density estimation for Pareto-based algorithms in many-objective optimization. *IEEE Transactions on Evolutionary Computation*, 18(3):348–365, 2014.

[13] H.-L. Liu, F. Gu, and Q. Zhang. Decomposition of a multiobjective optimization problem into a number of simple multiobjective subproblems. *IEEE Transactions on Evolutionary Computation*, 18(3):450 – 455, 2014.

[14] K. Miettinen. *Nonlinear multiobjective optimization*, volume 12 of *International Series in Operations Research and Management Science*. Kluwer Academic Publishers, 1999.

[15] R. C. Purshouse and P. J. Fleming. Evolutionary many-objective optimisation: An exploratory analysis. In *Proceedings of the IEEE Congress on Evolutionary Computation*, CEC'03, pages 2066–2073, 2003.

[16] H. Sato, H. E. Aguirre, and K. Tanaka. Controlling dominance area of solutions and its impact on the performance of MOEAs. In *Proceedings of the Conference on Evolutionary Multi-Criterion Optimization*, EMO'07, pages 5–20, 2007.

[17] T. Wagner, N. Beume, and B. Naujoks. Pareto-, aggregation-, and indicator-based methods in many-objective optimization. In *Proceedings of the Conference on Evolutionary Multi-Criterion Optimization*, EMO'07, pages 742–756, 2007.

[18] L. While, P. Hingston, L. Barone, and S. Huband. A faster algorithm for calculating hypervolume. *IEEE Transactions on Evolutionary Computation*, 10(1):29–38, 2006.

[19] S. Yang, M. Li, X. Liu, and J. Zheng. A grid-based evolutionary algorithm for many-objective optimization. *IEEE Transactions on Evolutionary Computation*, 17(5):721–736, 2013.

[20] E. Zitzler and S. Künzli. Indicator-based selection in multiobjective search. In *Proceedings of the Conference on Parallel Problem Solving from Nature*, PPSN'04, pages 832–842, 2004.

[21] E. Zitzler, M. Laumanns, and L. Thiele. SPEA2: Improving the strength pareto evolutionary algorithm. Technical Report 103, Computer Engineering and Networks Laboratory (TIK), ETH Zurich, Zurich, Switzerland, 2001.

[22] E. Zitzler and L. Thiele. Multiobjective optimization using evolutionary algorithms - A comparative case study. In *Proceedings of the Conference on Parallel Problem Solving From Nature*, PPSN'98, pages 292–304, 1998.

[23] E. Zitzler, L. Thiele, M. Laumanns, C. M. Fonseca, and V. G. da Fonseca. Performance assessment of multiobjective optimizers: An analysis and review. *IEEE Transactions on Evolutionary Computation*, 7(2), 2003.